Theor Chem Acc (2002) 107:282–290
DOI 10.1007/s00214-002-0332-3

Theoretical
Chemistry Accounts

Regular article

Dipole–reaction field interaction model for the solvent reorganization energy and its application to the benzoquinone–benzoquinone anion radical system

Xiang-Yuan Li, Quan Zhu, Lin-Lin Zhao, Shun-Qing Xiao, Feng Liu

College of Chemical Engineering, Sichuan University, Chengdu 610065, China

Received: 19 October 2001 / Accepted: 17 January 2002 / Published online: 3 May 2002

Abstract. Based on the spherical cavity approximation and the Onsager model, a dipole–reaction field interaction model has been proposed to elucidate the solvent reorganization energy of electron transfer (ET). This treatment only needs the cavity radius and the solute dipole moment in the evaluation of the solvent reorganization energy, and fits spherelike systems well. As an application, the ET reaction between *p*-benzoquinone and its anion radical has been investigated. The inner reorganization energy has been calculated at the level of MP2/6–31+G, and the solvent reorganization energies of different conformations have been evaluated by using the self-consistent reaction field approach at the HF/6–31+G level. Discussions have been made on the cavity radii and the values are found to be reasonable when compared with the experimental ones of some analogous intramolecular ET reactions. The ET matrix element has been determined on the basis of the two-state model. The fact that the value of the ET matrix element is about 10 times larger than *RT* indicates that this ET reaction can be treated as an adiabatic one. By invoking the classical Marcus ET model, a value of $4.9 \times 10^7 \mathrm{M}^{-1}\mathrm{s}^{-1}$ was obtained for the second-order rate constant, and it agrees quite well with the experimental one.

Key words: Dipole–reaction field interaction – Solvent reorganization energy – Electron-transfer matrix element – Rate constant

1 Introduction

Electron-transfer (ET) reactions between molecules and ions in solution have been the subject of a considerable number of experimental and theoretical studies during the past few decades. In the framework of Marcus ET theory, the rate constant, *k*, is given by [1]

$$k = \kappa A\sigma^2 \exp(-\Delta G^*/RT) \ , \quad (1)$$

with

$$\Delta G^* = \left(\lambda + \Delta G^0\right)^2/4\lambda \ , \quad (2)$$

where $A\sigma^2$ has the dimension of the collision frequency, σ is the average center-to-center distance in the reacting pair during the ET process, ΔG^* is the activation free energy, ΔG^0 is the "standard" reaction free energy and is zero for self-exchange, and λ is the reorganization energy composed of the inner reorganization energy, λ_i, and the solvent reorganization energy, λ_o, i.e.,

$$\lambda = \lambda_\mathrm{i} + \lambda_\mathrm{o} \ . \quad (3)$$

For the inner reorganization energy, both classical and quantum chemical calculations can be applied, while for the solvent reorganization energy, the dielectric continuum models are still predominant. In these models, the solvation is distinguished into two types: equilibrium and nonequilibrium solvation [2, 3, 4], and the solvent reorganization energy can be expressed as the free-energy difference between the nonequilibrium solvation and the equilibrium solvation, i.e.,

$$\lambda_\mathrm{o} = G_{\mathrm{n-eq}} - G_{\mathrm{eq}} \ , \quad (4)$$

where $G_{\mathrm{n\text{-}eq}}$ and G_{eq} are the nonequilibrium and the equilibrium free energy, respectively.

Generally, an equilibrium solvation state is defined as a state in which the total polarization of the solvent is equilibrated to the electronic charge distribution of the solute. It has attracted a great deal of attention during the past few decades, and many computer simulation methods at the ab initio level have been brought into practical applications. Among them, continuum models such as the polarizable continuum model (PCM) [5], the conductor-like screening model (COSMO) [6, 7, 8], the frequency-resolved cavity model (FRCM) [9, 10], and solvation models (SM*x*) [11, 12], are rather popular at present. These models assume that the solute molecule is placed in a cavity surrounded by the polarizable continuum, and that the continuum yields a charge distri-

---

Correspondence to: X.-Y. Li
e-mail: xyli@scu.edu.cn

bution on the cavity surface. However, different models treat the charge distribution in different ways. For example, the PCM considers the surface screening charges as a perturbation included in the Hamiltonian for the solute electronic structure calculations and performs a coupled iterative procedure until self-consistency is achieved; COSMO describes the solvent reaction field by means of apparent polarization charges distributed on the cavity surface and employs the boundary condition suited to the cavities in conductor media; FRCM subdivides the solvent reaction field into inertial and inertialess components associated with different cavities; while SM*x* divides physical effects into "electrostatics" and "first solvation shell effects" and estimates these two components through the parameterization of models.

Nonequilibrium solvation, however, has received far less attention and its calculation has remained somewhat unsatisfactory. Recently, there has been increasing interest in developing its theory, as well as in extending the conventional equilibrium reaction field methods to the nonequilibrium cases. In this work, we employ the theory developed by Lee, Kim, and Hynes [13, 14, 15, 16, 17]. It accounts for the relative time scales associated with the solute and solvent electronic motions via a coherent state representation for electronic polarization and a valence-bond description for the solute electronic structure, and gives some quantum mechanical description of molecular systems in solution undergoing nonequilibrium solvation.

The main aim of this work is to explore direct calculation for the solvent reorganization energy. Invoking Onsager reaction field model [18] and the point-dipole approximation, we have proposed the dipole–reaction field interaction model to describe the interaction between the solute and the solvent molecules and acquired a relationship between the solvent reorganization energy and the equilibrium electrostatic solvation free energy. This proportional relationship enables us to directly estimate the solvent reorganization energy. As an application, we have investigated the kinetic mechanics of ET reaction between *p*-benzoquinone (BQ) and its anion radical system. Such a choice is based on the following reasons: firstly, quinone-containing systems have the capacity to act as electron acceptors and thus they play a major role in ET reactions of photosynthesis and respiration [19, 20]; next, BQ can only form a weak hydrogen bond with its anion radical, hence the hydrogen-bonding interaction is weaker than the stacking interaction [21]; last, the symmetrical BQ molecules can only form a very limited number of different conformations of the dimer, and the experimental rate constant in solution is available [22, 23, 24, 25, 26, 27]. In addition, the structures and vibrational spectra of benzene dimers [23, 24], *p*-quinone dimers [21, 25], BQ and pyrimidine heterodimers [26] were investigated by using matrix-isolation IR spectroscopy by other authors, associated with ab initio calculations, and a conclusion was drawn that the stacked conformations are more stable than the planar ones. This is very important since the stacked conformations fit the spherical assumption of the Onsager model quite well. Hence, in our present work, we have paid attention only to the stacked conformations and compared the theoretical results with those available in the literature.

The outline of this article is as follows. We describe the nonequilibrium solvation free energy and establish the relationship between the solvent reorganization energy and the equilibrium electrostatic solvation free energy in Sect. 2. The theoretical results and corresponding discussions are presented in Sect. 3. Our conclusions are collected in Sect. 4.

2 Theoretical fundamentals

2.1 Equilibrium solvation free energy and self-consistent-reaction-field scheme

In the dielectric continuum model, when all the fields are assumed to be longitudinal, the free-energy functional for the solute electronic wave function, Ψ, can be expressed as [28]

$$G = \langle\psi|H_0|\psi\rangle - 1/2\int_v (P_e + P_{or})E_\psi(r, \rho^P)\mathrm{d}^3r + 1/2\int_v P_{or}\left[E_\psi(\rho^r, \sigma_e^r, \sigma_{or}^r) - E_\psi(\rho^P, \sigma_e, \sigma_{or}^r)\right]\mathrm{d}^3r \ . \quad (5)$$

In Eq. (5), H_0 is the vacuum Hamiltonian of the isolated solute, P_e and P_{or} are the electronic polarization and the orientational polarization, respectively, $E_\psi(r,\rho)$ is the electric field due to the solute charge distribution, ρ, of electronic state ψ in a vacuum, $E_\psi(\rho,\sigma_e,\sigma_{or})$ is the electric field resulting from the solute surface charge distribution σ_e from P_e and σ_{or} from P_{or} in solution. We denote the charge distribution as ρ^r before ET and ρ^p after ET within the cavity, and use r and p to refer to the reactant and the product states of ET, respectively, throughout of this article.

When the system is in equilibrium ($\rho^r = \rho^p$), the last integral in Eq. (5) vanishes and the expression of the equilibrium free energy is

$$G_{eq} = \langle\psi|H_0|\psi\rangle - 1/2\int_V (P_e + P_{or})E_\psi(r, \rho^r)\mathrm{d}^3r \ . \quad (6)$$

Clearly, in the case of P_e and P_{or} being in the same direction, Eq. (6) becomes

$$G_{eq} = \langle\psi|H_0|\psi\rangle - \frac{(\varepsilon_0 - 1)}{2(\varepsilon_0 - \varepsilon_\infty)}\int_V P_{or}(r)E_\psi(r, \rho^r)\mathrm{d}^3r \ . \quad (7)$$

The relationship of $P_e(r)/P_{or}(r) = \chi_e/\chi_{or}$ and the definitions $\chi_e = (\varepsilon_0 - 1)/4\pi$ and $\chi_{or} = (\varepsilon_0 - \varepsilon_\infty)/4\pi$ are used in the derivation of Eq. (7). Here ε_∞ is the solvent optical dielectric constant and ε_0 the solvent static dielectric constant.

In the self-consistent-reaction-field (SCRF) scheme associated with the Onsager model [5, 29, 30], the solute is embedded in a spherical cavity with radius a_0 surrounded by the continuous medium of dielectric constant ε_0. The dipole of the solute molecule will induce the solvent molecules to form a reaction field, R, and then the induced reaction field will in turn interact with the solute molecule dipole. By solving the Fock equation [31] and considering the solvent effect as a perturbation, we can get the expression of the energy of a solute, G_s, as

$$G_s = \langle\psi|H|\psi\rangle = \langle\psi|H_0\psi\rangle - \mu R \ , \tag{8}$$

where μ is the point dipole of the solute. R is proportional to the dipole moment i.e., $R = g\mu$, and the index g depends on both ε_0 and a_0, i.e. [18]

$$\mathrm{g} = 2(\varepsilon_0 - 1)/\left[(2\varepsilon_0 + 1)a_0^3\right] \ . \tag{9}$$

When the solvent polarization energy is included, the free energy of the system is given by [32]

$$G_{\mathrm{eq}} = G_s + \mu R/2 = \langle\psi|H_0|\psi\rangle - \mu R/2 \ . \tag{10}$$

On the other hand, it is well established that in molecular orbital theory, the total energy of a system can be expressed as the energy of the solute in a vacuum plus the equilibrium electrostatic solvation free energy, $\Delta G_{\mathrm{sol}}^{\mathrm{eq}}$, i.e. [5, 33]

$$G_{\mathrm{eq}} = \langle\psi|H_0|\psi\rangle + \Delta G_{\mathrm{sol}}^{\mathrm{eq}} \ . \tag{11}$$

Consequently, by comparing Eq. (11) with Eqs. (7) and (10), one can express the equilibrium electrostatic solvation free energy as follows:

$$\Delta G_{\mathrm{sol}}^{\mathrm{eq}} = -\frac{(\varepsilon_0 - 1)}{2(\varepsilon_0 - \varepsilon_\infty)} \int\limits_V P_{\mathrm{or}}(r) E_\psi(r, \rho^{\mathrm{r}})\mathrm{d}^3 r = -\mu R/2 \ . \tag{12}$$

Apparently, $\Delta G_{\mathrm{sol}}^{\mathrm{eq}}$ is proportional to the product of the solute dipole moment and the reaction field resulting from the medium polarization. If the nonequilibrium solvation free energy takes a form similar to the equilibrium one, or alternatively, the solvent reorganization energy can be expressed in terms of the dipole and the reaction field, the direct calculation of the solvent reorganization energy will be achieved. So in the following section, we determine the expressions of the nonequilibrium free energy and the solvent reorganization energy.

2.2 Nonequilibrium solvation and solvent reorganization energy

In solution, the solvent electronic motions are so fast that the electronic polarization can quickly adjust itself to any changes in the system and thus maintain its equilibrium character. The arrangements of the solvent nuclei, however, are much slower, and the orientational polarization usually cannot follow the rapid changes of charge distribution in the ET system. Therefore it is obvious that the nonequilibrium solvation needs different descriptions.

Provided that the solvent electronic polarization is equilibrated to both the electron and the solvent orientational polarization, in other words, P_{e} satisfies the Born–Oppenheimer approximation, we therefore have the following expression (Eq. 2.7 of Ref. [14]):

$$P_{\mathrm{e}}(r) = \chi_{\mathrm{e}} E_\psi(r, \rho P) - \chi_{\mathrm{e}} \int\limits_V T(r, r')[P_{\mathrm{e}}(r') + P_{\mathrm{or}}(r')]\mathrm{d}^3 r' \ . \tag{13}$$

In this work, we employ a multipole expansion [16], instead of the form in our previous work [34], and use the superscripts *lm* to denote the *lm*-pole component of the field, and obtain the following relation by eliminating the P_{e} degrees of freedom [16]

$$\left(\frac{1}{\chi_{\mathrm{el}}} + \frac{4\pi(l+1)}{2l+1}\right) P_{\mathrm{e}}^{lm}(r) = -\frac{4\pi(l+1)}{2l+1} P_{\mathrm{or}}^{lm} + E_\psi(r, \rho^{\mathrm{P}}) \ . \tag{14}$$

For the convenience of simplicity, we only consider the dipole and ignore the higher-order terms, take l as 1 and m as 0, and write Eq. (14) as

$$P_{\mathrm{e}}^{\mathrm{eq}}(r) = \frac{3(\varepsilon_\infty - 1)}{4\pi(2\varepsilon_\infty + 1)} E(r, \rho^{\mathrm{P}}) - \frac{2(\varepsilon_\infty - 1)}{2\varepsilon_\infty + 1} P_{\mathrm{or}} \ . \tag{15}$$

By replacing P_{e} in Eq. (5) with $P_{\mathrm{e}}^{\mathrm{eq}}(r)$ from Eq. (15), we can obtain the expression for the nonequilibrium free energy with a boundary condition, i.e.,

$$\begin{aligned} &G(\psi, P_{\mathrm{e}}^{\mathrm{eq}}[\psi, P_{\mathrm{or}}], P_{\mathrm{or}}) = \\ &\quad \langle\psi|H_0|\psi\rangle - \frac{3}{8\pi}\left(\frac{\varepsilon_\infty - 1}{2\varepsilon_\infty + 1}\right) \int\limits_V \left|E_\psi(r, \rho^{\mathrm{P}})\right|^2 \mathrm{d}^3 r \\ &\quad - \left(\frac{3}{2(2\varepsilon_\infty + 1)} + \frac{1}{2\varepsilon_\infty}\right) \int\limits_V P_{\mathrm{or}} E_\psi(r, \rho^{\mathrm{P}})\mathrm{d}^3 r + G_{\mathrm{or}} \ , \end{aligned} \tag{16}$$

where G_{or} is the self-free-energy associated with the orientational polarization. G_{or} is invariant in both the equilibrium and the nonequilibrium states. Its expression is

$$\begin{aligned} G_{\mathrm{or}} = &\frac{2\pi}{\varepsilon_0 - \varepsilon_\infty} \int\limits_V |P_{\mathrm{or}}|^2 \mathrm{d}^3 r \\ &+ \frac{1}{2\varepsilon_\infty} \int\limits_V \mathrm{d}^3 r \int\limits_V P_{\mathrm{or}} T(r, r') P_{\mathrm{or}}(r')\mathrm{d}^3 r' \ . \end{aligned} \tag{17}$$

According to Eq. (4), we can express the solvent reorganization energy as

$$\begin{aligned} \lambda_{\mathrm{o}} = &\left\langle\psi^P|H_0|\psi^P\right\rangle - \langle\psi^{\mathrm{r}}|H_0|\psi^{\mathrm{r}}\rangle \\ &- \frac{3}{8\pi}\frac{\varepsilon_\infty - 1}{2\varepsilon_\infty + 1} \int\limits_V \left(\left|E_\psi(r, \rho^{\mathrm{P}})\right|^2 - \left|E_\psi(r, \rho^{\mathrm{r}})\right|^2\right)\mathrm{d}^3 r \\ &- \left(\frac{3}{2(2\varepsilon_\infty + 1)} + \frac{1}{2\varepsilon_\infty}\right) \int\limits_V P_{\mathrm{or}}[E_\psi(r, \rho^{\mathrm{P}}) \\ &- E_\psi(r, \rho^{\mathrm{r}})]\mathrm{d}^3 r \ . \end{aligned} \tag{18}$$

The first and second terms in Eq. (18) are expectation values of the vacuum Hamiltonian in different electronic states ψ^{r} and ψ^{p}, while the last term is the difference of the interaction energy caused by the orientational polarization and the electric field associated with charge distribution, which is screened by the electronic polarization. In order to follow the Franck–Condon transition from ψ^{r} to ψ^{p}, the two expectation energy values should be degenerate at the ET transition state in the gas-phase case; thus,

$$\lambda_{\mathrm{o}}=-\frac{3}{8\pi}\frac{\varepsilon_\infty-1}{2\varepsilon_\infty+1}\int_V\left(\left|E_\psi(r,\rho^{\mathrm{P}})\right|^2-\left|E_\psi(r,\rho^{\mathrm{r}})\right|^2\right)\mathrm{d}^3r$$
$$-\left(\frac{3}{2(2\varepsilon_\infty+1)}+\frac{1}{2\varepsilon_\infty}\right)\int_V P_{\mathrm{or}}\left[E_\psi(r,\rho^{\mathrm{P}})-E_\psi(r,\rho^{\mathrm{r}})\right]\mathrm{d}^3r. \tag{19}$$

As far as a self-exchange ET is concerned, say, $\mathrm{B}^- + \mathrm{B} \rightarrow \mathrm{B} + \mathrm{B}^-$, we can safely assume that the solute has symmetric charge distributions before and instantly after ET at the position of the transition state; this means that the electric field produced by the solute charge distribution is approximately the same in magnitude and opposite in direction, i.e.,

$$E_\psi(r,\rho^{\mathrm{r}}) = -E_\psi(r,\rho^{\mathrm{P}}) \ , \tag{20}$$

$$\int_V \left|E_\psi(r,\rho^{\mathrm{r}})\right|^2\mathrm{d}^3r = \int_V \left|E_\psi(r,\rho^{\mathrm{P}})\right|^2\mathrm{d}^3r \ . \tag{21}$$

Therefore, combining Eq. (19) with Eqs. (20) and (21) gives

$$\lambda_{\mathrm{o}} = \left(\frac{3}{2\varepsilon_\infty+1}+\frac{1}{\varepsilon_\infty}\right)\int_V P_{\mathrm{or}}E_\psi(r,\rho^{\mathrm{r}})\mathrm{d}^3r$$
$$= -\frac{2(\varepsilon_0-\varepsilon_\infty)}{\varepsilon_0-1}\frac{5\varepsilon_\infty+1}{\varepsilon_\infty(2\varepsilon_\infty+1)}\Delta G_{\mathrm{sol}}^{\mathrm{eq}} \ . \tag{22}$$

Equation (22) establishes a relationship between λ_{o} and the equilibrium solvation energy, which enables us to calculate the reorganization energy of a self-exchange reaction by using the standard SCRF methods of arbitrary cavities. Equation (22) indicates that in self-exchange ET reactions, the solvent reorganization energy can be obtained by simply multiplying the equilibrium electrostatic solvation free energy by a proportional factor.

Under the condition of a spherical cavity and considering Eq. (12), we rewrite Eq. (22) as

$$\lambda_{\mathrm{o}} = \frac{(\varepsilon_0-\varepsilon_\infty)}{\varepsilon_0-1}\frac{5\varepsilon_\infty+1}{\varepsilon_\infty(2\varepsilon_\infty+1)}\mu R$$
$$= \frac{2(\varepsilon_0-\varepsilon_\infty)(5\varepsilon_\infty+1)}{\varepsilon_\infty(2\varepsilon_0+1)(2\varepsilon_\infty+1)a_0^3}\mu^2 \ . \tag{23}$$

Equation (23) indicates that the solvent reorganization energy is proportional to the product of the solute dipole and the reaction field, and thus we call this approach the dipole–reaction field interaction model. Since the equilibrium electrostatic solvation free energy can be evaluated through ab initio calculation with the SCRF, it is applicable to perform the direct estimation of the solvent reorganization energy.

For the solvent reorganization energy evaluation, there are also some other methods. Among them, the Lippert–Mataga relationship [16, 17, 35] is very popular. Its expression is

$$\lambda_{\mathrm{o}} = \left(\frac{\varepsilon_0-1}{2\varepsilon_0+1}-\frac{\varepsilon_\infty-1}{2\varepsilon_\infty+1}\right)\frac{1}{a_0^3}|\Delta\mu|^2 \ , \tag{24}$$

where $\Delta\mu$ is defined as the difference between the dipoles of the excited and ground states. This expression has been widely used in the description of absorption and emission spectra in solution for several decades. This expression will be used to validate Eq. (23).

3 Theoretical calculation

As an application, we perform the kinetic calculations of ET between BQ and its anion radical. From the experimental studies of Meisel and Fessanden [27], the rate constant was found to be in the range of $0.5\text{–}2 \times 10^8\ \mathrm{M}^{-1}\mathrm{s}^{-1}$. For the purpose of comparison, we calculated the inner and the solvent reorganization energies, the ET matrix element, as well as the reaction rate constant. The discussions are given in the relevant parts.

3.1 Geometry optimization

Owing to the $D_{2\mathrm{h}}$ symmetry, BQ is a very suitable model molecule for our studies since the BQ dimer only forms a very limited number of conformations. In accordance with other authors [21, 22, 23, 24, 25, 26], we focus on four conformations of BQ–BQ$^-$ encounter complexes: a parallel conformation, P, a crossing conformation, V, and two T-shaped conformations, T1 and T2 (shown in Fig. 1). In both stacked conformations P and V, the planes of BQ and BQ$^-$ are placed in a parallel way, with the axis through the two oxygen atoms in BQ and that in BQ$^-$ being oriented at 0° for P and 90° for V. The same axis is also oriented at 90° in the two T-shaped conformations, but the donor and the acceptor are placed in a perpendicular way, the BQ equilibrium geometry is placed at the top in conformation T1, while it is at the bottom in conformation T2 (Fig. 1c).

Since the Hartree–Fock (HF) self-consistent-field method is unable to describe the dispersion forces stabilizing the two aromatic rings in a stacked conformation [22], second-order Møller–Plesset perturbation theory (MP2) was employed in our theoretical calculations. However, owing to the computational intensity of Møller–Plesset perturbation calculations, their use is often restricted to "single-point" calculations at a geometry obtained using a lower level [36]. As a result, we initially optimized geometries of BQ and BQ$^-$ at the HF level with the 6-31G basis set augmented with the diffuse and polarization functions on both heavy atoms and hydrogen atoms (6-31++G**), and then performed the "single-point" calculation for the equilibrium geometries obtained at the MP2/6-31+G level. The bond parameters obtained at the level of HF/6-31++G** and the energies obtained at the level of MP2/6-31+G are listed in Table 1.

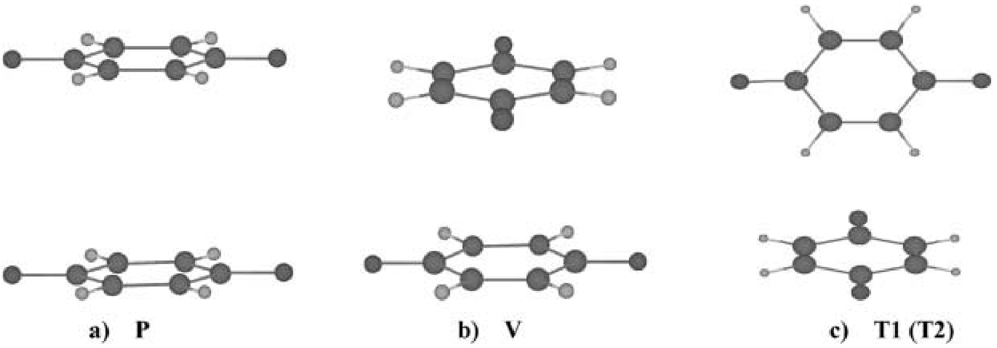
a) P b) V c) T1 (T2)

Fig. 1. Benzoquinone–benzoquinone anion radical conformations

On determining the stationary point of each conformation, a full optimization usually cannot give a reasonable donor–acceptor distance; the usual gradient optimization may lead to a false convergence owing to the weak interaction between the two moieties. To avoid this, we maintain the respectively optimized geometries of the donor and the acceptor and only investigate the dependency of the total energy upon the donor–acceptor distance under the constraint of C_{2v} symmetry. The equilibrium distance and the corresponding stabilization energy at the stationary point of each conformation were calculated at the level of MP2/6-31+G and are given in Table 2. It should be mentioned that we only focus on the donor–acceptor distances since this parameter is crucial in the further kinetic calculation of ET. Hence, no more precise treatment of the stabilization energy, for example, the basis set superposition error correction [37], was made in the present work.

3.2 Reorganization energy

3.2.1 Inner reorganization energy

Up to now, quantum chemistry calculations have been proved to be applicable and efficient in the evaluation of the inner reorganization energy. Although the ET reaction takes place in solution, the gas-phase inner reorganization energy might be a good approximation, because the bond parameters both in the gas phase and in solution are almost invariant. For a self-exchange ET reaction

$$B^- + B \rightarrow B + B^- \tag{25}$$

we can optimize the equilibrium geometries for B^- and B and thus obtain the corresponding equilibrium energies $E_{\mathrm{eq}}(B^-)$ and $E_{\mathrm{eq}}(B)$. On the other hand, we can calculate the energy $E_{\mathrm{n-eq}}(B)$ for neutral molecule B at the equilibrium configuration of B^-, but $E_{\mathrm{n-eq}}(B^-)$ for anion radical B^- at the equilibrium configuration of B. Thus, as shown in Fig. 2, we can obtain the inner reorganization energy through the energy calculation of the isolated species, i.e.,

$$\lambda_{\mathrm{i}}(B^-/B) = E_{\mathrm{n-eq}}(B^-) + E_{\mathrm{n-eq}}(B) - E_{\mathrm{eq}}(B^-) - E_{\mathrm{eq}}(B) \ . \tag{26}$$

At the MP2/6-31+G level, we performed the single-point calculations and obtained the value of 58.87 kJ mol^{-1} for λ_{i}.

3.2.2 Solvent reorganization energy

We used Eqs. (23) and (24) to evaluate the solvent reorganization energy. The only adjustable parameter is the cavity radius, a_0, and its choice has been the subject of many discussions [30]. We use here the value of the box occupied by the solute to approximate the cavity value, and thus to estimate the cavity radius. We first

Table 2. Total energy, E_t, and stabilization energy, E_s, of encounter complexes. d is the optimized distance between the mass centers of BQ and BQ$^-$, P_D and P_A are the total net charges on the donor and the acceptor, respectively, and $E_s = E_t(D) + E_t(A) - E_t(D...A)$ (kJ mol^{-1})

Conformation	d (nm)	P_D	P_A	E_t (au)	E_s (kJ mol^{-1})
P	0.3458	0.97	0.03	−759.78860	37.96
V	0.3312	0.98	0.02	−759.79616	57.80
T1	0.4912	0.97	0.03	−759.78907	39.19
T2	0.5023	1.00	0.00	−759.78352	24.61

Table 1. Optimized geometries of benzoquinone (*BQ*) and the benzoquinone anion radical (*BQ*$^-$). The bond lengths are in nanometers, the bond angles are in degrees, and the energy is in atomic units

	BQ			BQ$^-$	
	HF/631++G**	B3LYP[a]	Exp.[b]	HF/631++G**	B3LYP[a]
C_1O_3	0.1195	0.1218	0.1222	0.1248	0.1262
C_1C_7	0.1489	0.1486	0.1477	0.1443	0.1452
C_7C_8	0.1325	0.1339	0.1334	0.1360	0.1369
$C_8C_7C_1$	121.33	121.5	120.9	122.50	122.8
$C_7C_1C_5$	115.92	117.1	118.2	116.63	114.4
E_t^c		−379.85402			−379.92012

[a] From Ref. [38]
[b] From Ref. [39]
[c] Energies at the MP2/6−31+G level in this work

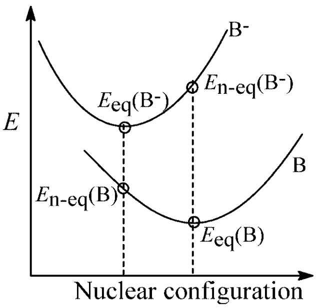

Fig. 2. A schematic description of the calculation of the inner reorganization energy

determine the smallest box enclosing the solute, plus the van der Waals radius of the hydrogen atom, so as to obtain cavity volume. Then, we estimate the cavity radius by using $a_0 = (3V_M/4\pi)^{1/3}$. By substituting the estimated cavity radii for a_0 in Eqs. (23) and (24) and taking $\varepsilon_\infty = 1.8$ and $\varepsilon_0 = 78.5$ [40] for aqueous solution, we can perform an SCRF calculation to obtain the solvent reorganization energies for those conformations shown in Fig. 1. Since only the solute dipole moment is needed, we performed this calculation at the HF/6-31+G level, rather than at the MP2/6-31+G level, since MP2 correction does not improve the dipole moment. In Eq. (24) we consider that the solute dipole only changes its direction after the Frank–Condon transition for a self-exchange reaction. The results are collected in Table 3.

On the other hand, according to Marcus' two-sphere model [1, 2, 3, 4], the solvent reorganization energy is expressed as

$$\lambda_o = \Delta e^2 \left(\frac{1}{2r_D} + \frac{1}{2r_A} - \frac{1}{d_{DA}} \right) \left(\frac{1}{\varepsilon_\infty} - \frac{1}{\varepsilon_0} \right) , \tag{27}$$

where Δe is the transferred charge, and r_D, r_A, and d_{DA} are the donor sphere radius, the acceptor sphere radius, and the ET distance, respectively. Since $\varepsilon_\infty = 1.8$ and $\varepsilon_0 = 78.5$ for aqueous solution, and $r_D = r_A = a$ in our case, by taking the units of a and d_{DA} in nanometers and λ_o in kilojoules per mole, we can simplify Eq. (27) to the following form:

$$a = \frac{76.592 d_{DA}}{d_{DA}(\lambda_0 + 76.592)} . \tag{28}$$

Using our values of λ_o from the SCRF calculation, we obtained the two-sphere radius a (Table 3). We see that the compact conformations P and V yield the smaller two-sphere radii, while the "loose" conformations T1 and T2 produce larger ones. Owing to the disorder of molecules in the liquid state, we take the average value of 0.318 nm for these four conformations as the estimate of the molecular radius. These values might be compared with the molecular radii calculated from the molar volume by using the equation [32]

$$(4/3)\pi a^3 = (M/\rho)N_0 , \tag{29}$$

where N_0 is Avogadro's number and ρ is the density of BQ, say 1.318 kg dm^{-3} [40]. The value of $a = 0.32$ nm so calculated testifies the suitability of our estimated cavity radii, and gives us confidence for the further use of the solvent reorganization energy. On the other hand, let us consider the Marcus two-sphere model for the estimation of the solvent reorganization energy instead of the single-sphere one used previously. From the value of our calculation or the density method, the radius of BQ is around 0.32 nm. However, the center-to-center distance of the complex is found to be much smaller than the sum of the donor and the acceptor radii. This means that there is overlap between these two spheres. In such cases, the two-sphere model (Eq. 27) no longer works well. Therefore, the single-sphere model used by us is possibly a better choice for those "compact" intramolecular systems.

At the same time, in order to compare our solvent reorganization energy with the experimental results, we also find some relevant results for ET reactions including BQ. The well-known Miller–Closs intramolecular systems [41, 42] are good examples. The solvent reorganization energy for the biphenyl anion and BQ system, as well as that for the 2-(9,9-dimethyl)fluorenyl anion and BQ system which is mediated by an organic spacer, were fitted from the observed rate constant. After cutting off the contribution from the low-frequency torsion motion around the central C–C bond in biphenyl, the solvent reorganization energy of both systems is around 50 kJmol^{-1}. These systems were also calculated by Newton et al. [10] with their FRCM, and the results obtained are about 45 kJmol^{-1}. Our results are in the range 46–67 kJmol^{-1}, and the average value is 58.54 kJmol^{-1}. Hence, we think our results are reasonable for the BQ–BQ$^-$ system, although we failed to find direct evidence from experimental measurements.

3.3 ET matrix element and the zero-overlap problem

Generally denoted as V_{rp}, in which r and p refers to the initial and final state, the ET matrix element, or equivalently the electronic coupling element, plays a key role in controlling the rates of many ET reactions. Consequently, over the past few decades, there have been significant efforts to determine this quantity both

Table 3. Cavity radii, dipole moments, solvent reorganization energies, and two-sphere radii

Structure	d (nm)	a_0 (nm)	μ (au)	λ_o (kJ mol^{-1})[a]	λ_o' (kJ mol^{-1})[b]	a (nm)
P	0.3458	0.432	3.1975	57.87	62.48	0.274
V	0.3312	0.447	2.9990	45.96	49.61	0.276
T1	0.4912	0.528	4.6259	66.34	71.62	0.345
T2	0.5023	0.526	4.5179	64	69.10	0.354

[a] Using Eq. (23)
[b] Using Eq. (24)

from experimental data and from quantum chemical calculations [43, 44]. For systems in the gas phase, reasonably good agreement between theory and experiment has been obtained, while for ET reactions in solution, a practical yet reliable approach, which allows incorporation of structure-dependent electronic coupling in their simulations, is still a major challenge for quantum chemistry [45]. Some authors, for example, Miller and coworkers, suggested that the solvent could cause a significant increase in the electronic coupling at a given donor–acceptor distance [46, 47], while others argued that if we only treat the transferring electron, the existence of solvent does not influence V_{rp} significantly, and thus the gas-phase calculation of this quantity might be a good approximation for that in solution [14, 45].

Up to the present, there have been several approaches to evaluating the ET matrix element, such as the generalized Mulliken–Hush (GMH) approach [48, 49], Koopmans' theorem (KT) [53, 54], and the variational treatment on electron-localized diabatic states [52, 53]. The GMH approach relates the ET element to the transition dipole moment between the states of interest, and this method is generally applied to investigate charge-transfer processes by using the diagonalization of the dipole moment matrix to define diabatic states. The KT method approximates the state–state energy splitting using the transition energy from one molecular orbital to another. In the present work, we evaluate V_{rp} from the direct variational treatment of the two electron-localized nonorthogonal states. The fundamentals of this treatment are given in the following paragraph.

As shown in Fig. 3, the ET matrix element is marked as half the energy splitting at the crossing of two diabatic electronic states η_{r} and η_{p}. The secular equation of the two-state problem is given as follows:

$$\begin{vmatrix} H_{\mathrm{rr}} - E & H_{\mathrm{rp}} - ES_{\mathrm{rp}} \\ H_{\mathrm{pr}} - ES_{\mathrm{pr}} & H_{\mathrm{pp}} - E \end{vmatrix} = 0 \ , \tag{30}$$

where H is the total electronic Hamiltonian and $H_{\mathrm{ij}} = \eta_{\mathrm{i}}|H|\eta_{\mathrm{j}}>$, and S is the overlap integral of the two diabatic state, i.e., $S_{\mathrm{ij}} = \langle \eta_{\mathrm{i}}|\eta_{\mathrm{j}}\rangle$, $(i,j = \mathrm{r,p})$. By representing the potential energies of the two adiabatic states at the avoided crossing as E_+ and E_-, respectively, V_{rp} can be given by

$$V_{\mathrm{rp}} = (E_+ - E_-)/2 = \left(1 - S_{\mathrm{rp}}^2\right)^{-1} \left|H_{\mathrm{rp}} - S_{\mathrm{rp}}\left(H_{\mathrm{rr}} + H_{\mathrm{pp}}\right)/2\right| \ . \tag{31}$$

For our BQ–BQ$^-$ self-exchange reaction, η_{r} and η_{p} are degenerate energetically at the transition state. By introducing what used to be called the linear reaction coordinate [52], we can obtain two charge-localized states at the crossing of the two diabatic potential-energy surfaces, and then employ the HONDO99 [54] program to calculate V_{rp} for each conformation shown in Fig. 1.

From Table 4, we see that the P conformation gives a normal value of V_{rp}, whereas trouble emerges in the V, T1, and T2 ones and V_{rp} tends to be infinite. Such a result is in fact not strange since the so-called "pseudo-orthogonality" occurs in these cases [55]. In the subroutines linked to HONDO developed by Farazdel and Dupuis [54, 56], for the sake of convenience in the derivation, the overlap, S_{rp}, between η_{r} and η_{p} is treated as a "prod" factor and is used as the denominator in the calculation. However, when "pseudo-orthogonality" occurs in a system, there is zero overlap between η_{r} and η_{p} and thus "prod" is zero; thus, ordinary treatment leads to an infinite value of V_{rp}. To solve this problem, one of the authors developed another procedure, which differs from what was coded in HONDO, and gave the final expression by Eq. (13) in Ref. [55]. A few subroutines were added to the HONDO program. After the calculations, all the values of S_{rp} for conformations V, T1, and T2 are zero, and finite values of V_{rp} are obtained (Table 4).

An alternative approach to the zero values of V_{rp} is to show that η_{r} and η_{p} belong to different irreducible representations according to the symmetry applied. When BQ and BQ$^-$ are placed in the stacked conformation, the encounter complex in each stacked conformation has C_{2v} symmetry. The symmetries of the diabatic states η_{r} and η_{p} are also collected in Table 4, and we can see that the irreducible representations of η_{r} and η_{p} for the V, T1, and T2 structures differ from each other and the analyses are consistent with our direct calculation.

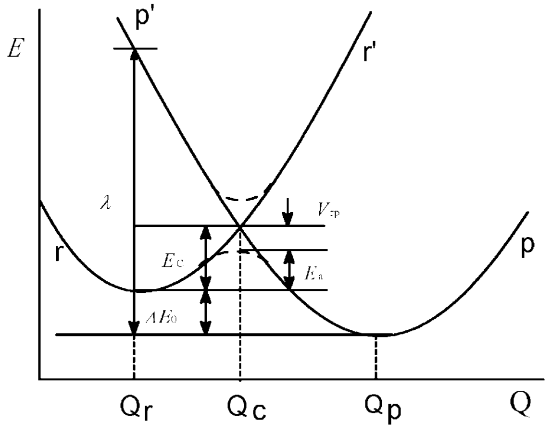

Fig. 3. Double-well potential of the electron-transfer reaction in the Marcus normal region

3.4 ET reaction rate constant

From Table 4, we can see that the ET is only efficient for the P-type conformation since the zero value of V_{rp} in

Table 4. Electron-transfer matrix element at the UHF/6-31+G level

	Conformation			
	P	V	T1	T2
Symmetry of η_{r}	B_1	B_1	A_2	B_1
Symmetry of η_{p}	B_1	B_2	B_2	A_1
S_{rp}	0.1779	0	0	0
V_{rp} (kJmol^{-1})	16.29	0	0	0

the other three conformations implies that there is no transition from the initial state to the final one. In addition, the relatively large V_{rp} value of the P-type conformation indicates that we can handle this system by using Marcus adiabatic ET theory. Combining Eq. (1) with the self-exchange reaction $\mathrm{BQ}^- + \mathrm{BQ} \xrightarrow[k_{-\mathrm{d}}]{k_{\mathrm{d}}} \mathrm{BQ}^- \cdots \mathrm{BQ} \xrightarrow{k_{\mathrm{et}}} \mathrm{BQ} \cdots \mathrm{BQ}^- \rightarrow \mathrm{BQ} + \mathrm{BQ}^-$, and applying the steady-state approximation, we may express the second-order rate constant as [57]

$$k_{\mathrm{obs}} = \frac{k_{\mathrm{d}}}{1 + k_{\mathrm{d}} k_{-\mathrm{d}} / k_{\mathrm{et}} k_{\mathrm{d}}} \quad . \tag{32}$$

Associated with Eyring's equation, the final expression of the observed rate constant reads

$$k_{\mathrm{obs}} = \frac{k_{\mathrm{d}}}{1 + \frac{k_{\mathrm{d}}}{k_{\mathrm{d}} Z} k_{\mathrm{d}} \exp(\Delta G^* / RT)} \quad . \tag{33}$$

In general, one can take $k_{-\mathrm{d}}/k_{\mathrm{d}}$, k_{d}, and Z as 1 M^{-1}, 2×10^{10} $\mathrm{M}^{-1}\mathrm{s}^{-1}$, and 6.2×10^{12} s^{-1}, respectively. As we know, for the self-exchange, $\Delta G^0 = 0$. By replacing λ with the sum of our results, say, 58.87 kJmol^{-1} for λ_{i} and 57.87 kJmol^{-1} for λ_{o}, and taking the temperature as 298.15 K, the second-order rate constant of our selected P conformation is predicted to be 4.9×10^7 $\mathrm{M}^{-1}\mathrm{s}^{-1}$. Compared with the experimental value of 6.2×10^7 $\mathrm{M}^{-1}\mathrm{s}^{-1}$ [27], our result is pretty satisfactory.

4 Conclusion

In this article, we have detailed the expressions of the equilibrium free energy, the equilibrium electrostatic solvation free energy, and the nonequilibrium free energy. Through necessary derivations, we have established a relationship between the solvent reorganization energy and the equilibrium electrostatic solvation free energy (Eq. 22). By employing the Onsager reaction field theory, we have achieved a very condensed form which contains only one adjustable parameter. Apparently, our dipole–reaction field interaction model permits the direct evaluation for the solvent reorganization energy by performing a SCRF calculation.

As an application, we have investigated ET between BQ and its anion radical. Four conformations were taken into account. After performing theoretical calculations of the inner and the solvent reorganization energies, we discussed the validity of the dipole–reaction field interaction model. Agreement between our estimated two-sphere radius and that calculated from the density, as well as the consistency between our solvent reorganization energies and the experimental ones of some analogous intramolecular systems, gives us confidence to apply our model to spherelike systems. Calculations of the ET matrix element were also made, and only the stacked P conformation gives a nonzero V_{rp}. In conformations V, T1, and T2, there is the "pseudo-orthogonality" problem, and two approaches were given to explain it. Since the value of V_{rp} is found to be about 10 times larger than RT, which indicates a large interaction between the two diabatic states, we are encouraged to apply the classical Marcus theory. The second-order rate constant from our calculations agrees quite well with the experimentally observed one.

All the ab initio calculations were carried out with the HONDO99 package [54].

Acknowledgements. This work was supported by the National Natural Science Foundation of China (29892164, 39970183) and the State Key Laboratory of Theoretical and Computational Chemistry in Jilin University. The authors thank Michel Dupuis for his help in making use of the HONDO program.

References

1. Marcus RA (1993) Angew Chem Int Ed Engl 32: 1111
2. Marcus RA (1956) J Chem Phys 24: 966
3. Marcus RA (1963) J Phys Chem 67: 853
4. Marcus RA (1965) J Chem Phys 43: 679
5. Tomasi J, Persico M (1994) Chem Rev 94: 2027
6. Klamt A, Schuurmann G (1993) J Chem Soc Perkins Trans 2: 799
7. Andzelm J, Kolmel C, Klamt A (1995) J Chem Phys 103: 9312
8. Barone V, Cossi M (1998) J Phys Chem A 102: 1995
9. Basilevsky MV, Rostov IV, Newton MD (1998) Chem Phy 232: 189
10. Newton MD, Basilevsky MV, Rostov IV (1998) Chem Phys 232: 201
11. Chambers CC, Hawkins GD, Cramer CJ, Truhlar DG (1996) J Phys Chem 100: 16385
12. Hawkins GD, Cramer CJ, Truhlar DG (1997) J Phys Chem B 101: 7147
13. Lee S, Hynes JT (1988) J Chem Phys 88: 6853
14. Kim HJ, Hynes JT (1990) J Chem Phys 93: 5194
15. Kim HJ, Hynes JT (1992) J Chem Phys 96: 5088
16. Kim HJ (1996) J Chem Phys 105: 6818
17. Kim HJ (1996) J Chem Phys 105: 6833
18. Onsager L (1936) J Am Chem Soc 58: 1486
19. Hobza P, Selzle HL, Schlag EW (1993) J Phys Chem 97: 3937
20. Rubio M, Torrens F, Sanchez-Marin J (1993) J Comput Chem 14: 647
21. Plokhotnichenko AM, Radchenko ED, Stepanian SG, Adamowicz L (1999) J Phys Chem A 103: 11052
22. Yoshihara T, Yamaji M, Itoh T, Shizuk H, Shimokage T, Tero-Kubota S (2000) Phys Chem Chem Phys 2: 993
23. Hobza P, Selzle HL, Schlag EW (1994) J Am Chem Soc 116: 3500
24. Hobza P, Selzle HL, Schlag EW (1990) J Chem Phys 93: 5893
25. McCarthy W, Plokhotnichenko AM, Radchenko ED, Smets J, Smith DMA, Stepanian SG, Adamowicz L (1997) J Phys Chem A 101: 7208
26. Cook AR, Curtiss LA, Miller JR (1997) J Am Chem Soc 119: 5729
27. Meisel D, Fessenden RW (1976) J Am Chem Soc 98: 7505
28. Aguilar MA, Olivares del Valle FJ, Tomasi J (1993) J Chem Phys 98: 7375
29. Kestner NR, Logan J, Jortner J (1974) J Phys Chem 78: 2148
30. Tapia O, Goscinski O (1975) Mol Phys 29: 1653
31. Wong MW, Frisch MJ, Wiberg KB (1991) J Am Chem Soc 113: 4776
32. Karelson MM, Katritzky AR, Szafran M, Zerner M (1989) J Org Chem 54: 6030
33. Maus M, Rettig W, Depaemelaere S, Onkelinx A, Schryver FCD, Iwai K (1998) Chem Phys Lett 292: 115
34. Li X-Y, Zhao L-L, Xiao S-Q (2000) Theor Chem Acc 105: 78
35. van der Zwan G, Hynes JT (1985) J Phys Chem 89: 4181
36. Leach AR (1996) Molecular modelling: principles and applications. Addison Wesley Longman, London, p 85
37. FB van Duijneveldt, JGCM van Duijneveldt-van de Rijdt, JH van Lenthe (1994) Chem Rev 94: 1873
38. Eriksson LA, Himo F, Siegbahn PEM, Babcock GT (1997) J Phys Chem A 101: 9496

39. Brown MA, McGarvey BR, Tuck DG (1998) J Chem Dalton Trans 1371
40. Dean JA (1999) Lange's handbook of chemistry, 15th edn. McGraw-Hill, New York, p 5.134
41. Closs GL, Calcaterra LT, Green NJ, Penfield KW, Miller JR (1986) J Phys Chem 90: 3673
42. Miller JR, Paulson BP, Bal R, Closs GL (1995) J Phys Chem 99: 6923
43. Larsson S, Volosov A (1986) J Chem Phys 85: 2548
44. Paulson BP, Curtiss LA, Bal B, Closs GL, JR Miller (1996) J Am Chem Soc 118: 378
45. Warshel A, Parson WW (1991) Annu Rev Phys Chem 42: 279
46. Henderson TM, Cave RJ (1998) J Chem Phys 109: 7414
47. Miller NE, Wander MC, Cave RJ (1999) J Phys Chem A 103: 1084
48. Cave RJ, Newton MD (1997) J Chem Phys 106: 9213
49. Cave RJ, Newton MD (1996) Chem Phys Lett 249: 15
50. Rodriguez-Monge L, Larsson S (1996) J Phys Chem 100: 6298
51. Li X-Y, He F-C (2000) J Comput Chem 20: 597
52. Farazdel A, Dupuis M, Clementi E, Aviram A (1990) J Am Chem Soc 112: 4206
53. Zhang LY, Friesner RA, Murphy RB (1997) J Chem Phys 107: 450
54. Dupuis M, Marquez A, Davidson ER (1999) HONDO 99, based on HONDO 95.3, Dupuis M, Marquez A, Davidson ER, Quantum Chemistry Program Exchange, Indiana University, Bloomington, p 47405
55. Li XY, Tian AM, He FC, Yan GS (1996) J Comput Chem 17: 1108
56. Farazdel A, Dupuis M, Clementi E (1990) Modern techniques in computational chemistry: MOTECC-90. IBM Corporation, Kington, NY, p 324
57. Eberson L (1987) Electron transfer reactions in organic chemistry. Springer, Berlin Heidelberg New York, p 30